# Motor Bearing Damage Detection Using Stator Current Monitoring

Randy R. Schoen, *Member, IEEE,* Thomas G. Habetler, *Senior Member, IEEE,*
Farrukh Kamran, *Student Member, IEEE,* and Robert G. Bartheld, *Senior Member, IEEE*

*Abstract*—**This paper addresses the application of motor current spectral analysis for the detection of rolling-element bearing damage in induction machines. Vibration monitoring of mechanical bearing frequencies is currently used to detect the presence of a fault condition. Since these mechanical vibrations are associated with variations in the physical air gap of the machine, the air gap flux density is modulated and stator currents are generated at predictable frequencies related to the electrical supply and vibrational frequencies. This paper takes the initial step of investigating the efficacy of current monitoring for bearing fault detection by correlating the relationship between vibration and current frequencies caused by incipient bearing failures. The bearing failure modes are reviewed and the characteristic bearing frequencies associated with the physical construction of the bearings are defined. The effects on the stator current spectrum are described and the related frequencies determined. This is an important result in the formulation of a fault detection scheme that monitors the stator currents. Experimental results which show the vibration and current spectra of an induction machine with different bearing faults are used to verify the relationship between the vibrational and current frequencies. The test results clearly illustrate that the stator current signature can be used to identify the presence of a bearing fault.**

## I. Introduction

RECENTLY, motor reliability studies have been performed by both General Electric, under the sponsorship of the Electric Power Research Institute [1], and the IEEE Industry Applications Society [2] in order to evaluate the reliability of electric motors and identify design and operational characteristics that offer the potential to increase their reliability. These studies specifically apply to machines, 100 hp or more, that are operated in industrial and commercial installations. The results of these studies show that bearing problems account for over 40% of all machine failures. Over the past several decades, rolling-element (ball and roller) bearings have been utilized in many electric machines while sleeve (fluid-film) bearings are installed in only the largest industrial machines. In the case of induction motors, rolling-element bearings are overwhelmingly used to provide rotor support.

In many situations, vibration monitoring methods are utilized to detect the presence of an incipient bearing failure. However, it has been suggested [3]–[5] that stator current monitoring can provide the same indications without requiring access to the motor. This paper demonstrates the feasibility of this detection method by correlating the characteristic bearing frequencies to the spectral components of the stator current. Test results showing the vibration and current spectrums are used to clearly exhibit this relationship.

## II. Bearing Failure Causes

Rolling-element bearings generally consist of two rings, an inner and outer, between which a set of balls or rollers rotate in raceways. Under normal operating conditions of balanced load and good alignment, fatigue failure begins with small fissures, located below the surfaces of the raceway and rolling-elements, which gradually propagate to the surface generating detectable vibrations and increasing noise levels [6]. Continued stressing causes fragments of the material to break loose producing a localized fatigue phenomena known as flaking or spalling [6], [7]. Once started, the affected area expands rapidly contaminating the lubrication and causing localized overloading over the entire circumference of the raceway [6]. Eventually the failure results in rough running of the bearing. While this is the normal mode of failure in rolling-element bearings, there are many other conditions which reduce the time of bearing failure. These external sources include contamination, corrosion, improper lubrication, improper installation, or brinelling.

Contamination and corrosion frequently accelerate bearing failure because of the harsh environments present in most industrial settings. Dirt and other foreign matter that is commonly present often contaminate the bearing lubrication. The abrasive nature of these minute particles, whose hardness can vary from relatively soft to diamond-like, cause pitting and sanding actions that give way to measurable wear of the balls and raceways [7]. Bearing corrosion is produced by the presence of water, acids, deteriorated lubrication, and even perspiration from careless handling during installation [6], [7]. Once the chemical reaction has advanced sufficiently, particles are worn off resulting in the same abrasive action produced by bearing contamination.

Paper IPCSD 95–45, approved by the Electric Machines Committee of the IEEE Industry Applications Society for presentation at the 1994 Industry Applications Society Annual Meeting, Denver, CO, October 2–7. This work was supported by a Georgia Tech research contract with Siemens Energy and Automation, Inc. Manuscript released for publication May 23, 1995.

R. R. Schoen, T. G. Habetler, and F. Kamran are with the School of Electrical and Computer Engineering, Georgia Institute of Technology, Atlanta, GA 30332-0250 USA.

R. G. Bartheld is with Siemens Energy & Automation, Inc., Atlanta, GA 30356-9000 USA.

IEEE Log Number 9414523.

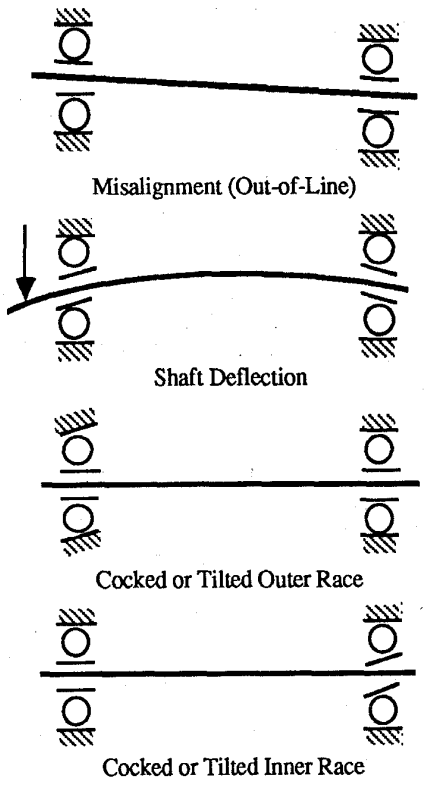


Fig. 1. Four types of rolling-element bearing misalignment [7].

Improper lubrication includes both under- and over-lubrication. In either case, the rolling-elements are not allowed to rotate on the designed oil film causing increased levels of heating. The excessive heating causes the grease to break down which reduces its ability to lubricate the bearing elements and accelerates the failure process.

Installation problems are often caused by improperly forcing the bearing onto the shaft or in the housing. This produces physical damage in the form of brinelling or false brinelling of the raceways which leads to premature failure. Misalignment of the bearing, which occurs in the four ways depicted in Fig. 1, is also a common result of defective bearing installation. The most common of these is caused by tilted races [7].

Brinelling is the formation of indentations in the raceways as a result of deformation caused by static overloading. While this form of damage is rare, a form of "false brinelling" occurs more often. In this case, the bearing is exposed to vibrations while stationary. Even though lightly loaded bearings are less susceptible, false brinelling still happens and has even occurred during the transportation of uninstalled bearings [6].

Regardless of the failure mechanism, defective rolling-element bearings generate mechanical vibrations at the rotational speeds of each component. These characteristic frequencies, which are related to the raceways and the balls or rollers, can be calculated from the bearing dimensions and the rotational speed of the machine. Mechanical vibration analysis techniques are commonly used to monitor these frequencies in order to determine the condition of the bearing.

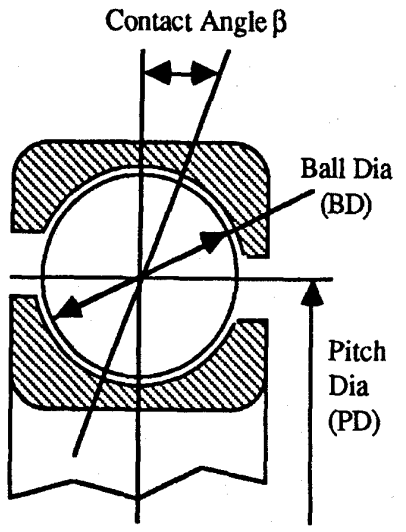


Fig. 2. Ball bearing dimensions.

## III. Current Spectrum Effects

The relationship of the bearing vibration to the stator current spectrum can be determined by remembering that any air gap eccentricity produces anomalies in the air gap flux density [8]. In the case of a dynamic eccentricity that varies with rotor position, the oscillation in the air gap length causes variations in the air gap flux density. This, in turn, affects the inductances of the machine producing stator current harmonics with frequencies predicted by [4], [5]

$$f_{ecc} = f_e \left[ 1 \pm k \left( \frac{1-s}{\frac{p}{2}} \right) \right] = |f_e \pm k \cdot f_{rm}| \quad (1)$$

where $f_e$ is the electrical supply frequency, $k = 1, 2, 3, \cdots, s$ is the per unit slip, $p$ is the number of machine poles, and $f_{rm}$ is the mechanical rotor speed in Hertz.

Since ball bearings support the rotor, any bearing defect will produce a radial motion between the rotor and stator of the machine. The mechanical displacement resulting from the damaged bearing causes the air gap of the machine to vary in a manner that can be described by a combination of rotating eccentricities moving in both directions, i.e., clockwise and counterclockwise. As with the air gap eccentricity, these variations generate stator currents at predictable frequencies, $f_{bng}$, related to the vibrational and electrical supply frequencies by

$$f_{bng} = |f_e \pm m \cdot f_v| \quad (2)$$

where $m = 1, 2, 3, \cdots$ and $f_v$ is one of the characteristic vibration frequencies.

The characteristic frequencies for ball bearings are based upon the bearing dimensions shown in Fig. 2. In radially loaded bearings, the contact areas of the balls and raceways carry the heaviest loads causing most fatigue failures to involve these components [9]. The ball spin frequency is caused by the rotation of each ball about its center. Since a defect on a ball will contact with both the inner and outer races

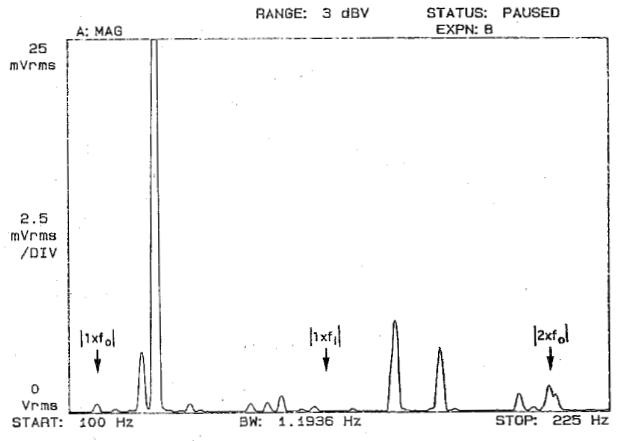


Fig. 3. Vibration spectrum (acceleration) of loaded 4-pole induction machine with a hole in the outer race of the shaft-end bearing (100–225 Hz).

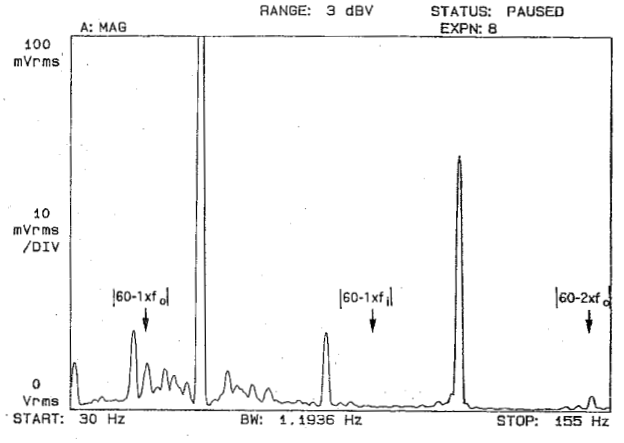


Fig. 4. Stator current spectrum of loaded 4-pole induction machine with a hole in the outer race of the shaft-end bearing (30–155 Hz).

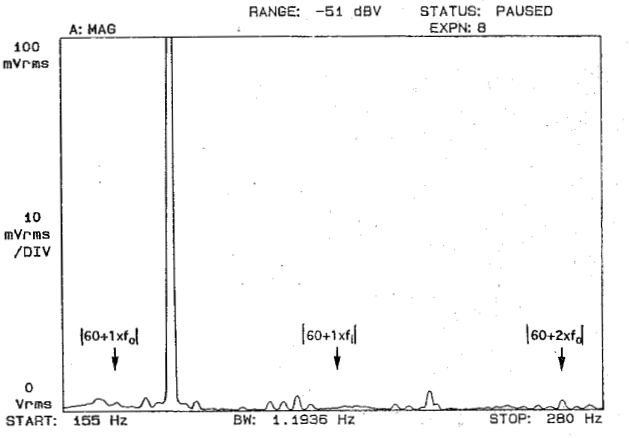


Fig. 5. Stator current spectrum of loaded 4-pole induction machine with a hole in the outer race of the shaft-end bearing (155–280 Hz).

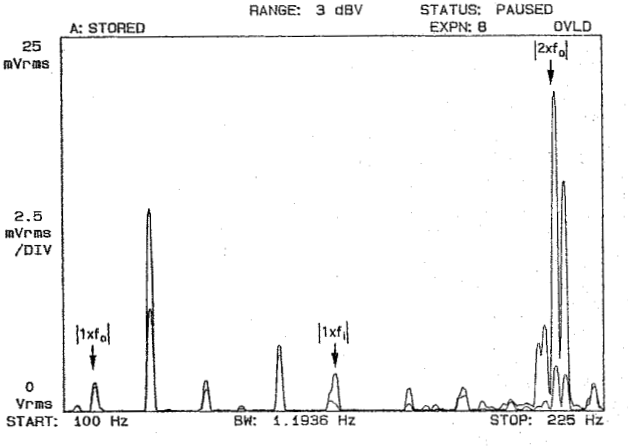


Fig. 6. Vibration spectrum (acceleration) of unloaded 4-pole induction machine with brinelling of both bearings (100–225 Hz).

during every revolution, the ball defect frequency is twice the spin frequency and can be written as

$$f_b = \frac{PD}{BD} f_{rm} \left[ 1 - \left( \frac{BD}{PD} \cos \beta \right)^2 \right] \tag{3}$$

where $PD$ is the bearing pitch diameter, $BD$ is the ball diameter, $\beta$ is the contact angle of the balls on the races, and $f_{rm}$ is the mechanical rotor speed in Hertz. The outer and inner raceway frequencies are produced when each ball passes over a defect. This occurs $n$-times during a complete circuit of the raceway where $n$ is the number of balls. This causes the outer and inner race frequencies to be defined as

$$f_o = \frac{n}{2} f_{rm} \left[ 1 - \frac{BD}{PD} \cos \beta \right] \tag{4}$$

$$f_i = \frac{n}{2} f_{rm} \left[ 1 + \frac{BD}{PD} \cos \beta \right]. \tag{5}$$

Bearing cage faults generally bind the balls producing skidding and slipping along the raceway. These effects cause high frequency vibrations to be generated.

It should be noted from (4) and (5) that specific information concerning the bearing construction is required to calculate the exact characteristic frequencies. However, these characteristic race frequencies can be approximated for most bearings with between six and twelve balls by [10]

$$f_o = 0.4 \cdot n \cdot f_{rm};$$
$$f_i = 0.6 \cdot n \cdot f_{rm}. \tag{6}$$

This generalization allows for the definition of frequency bands where the bearing race frequencies are likely to show up without requiring explicit knowledge of the bearing construction. Therefore, it is possible to formulate an effective fault detection scheme which monitors the related stator current spectrum for bearing defects.

## IV. Experimental Test Results

In order to relate the bearing vibrations to the stator current spectrum, a hole was drilled through the outer race of the shaft-end bearing (NSK 6208) of a four-pole test motor. While this is not a realistic bearing failure, the nature of the fault produces bearing frequencies that are isolated to the outer race and are easily located in the vibration and current spectrums. From the bearing data sheet, the outside diameter of the 6208 bearing is 80 mm and the inside diameter is 40 mm. Assuming that

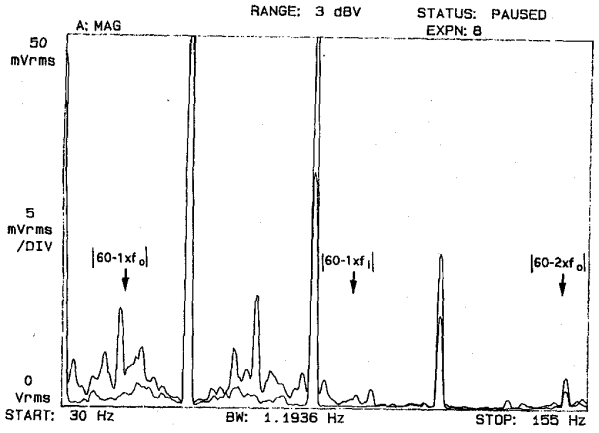


Fig. 7. Stator current spectrum of unloaded 4-pole induction machine with brinelling of both bearings (30–155 Hz).

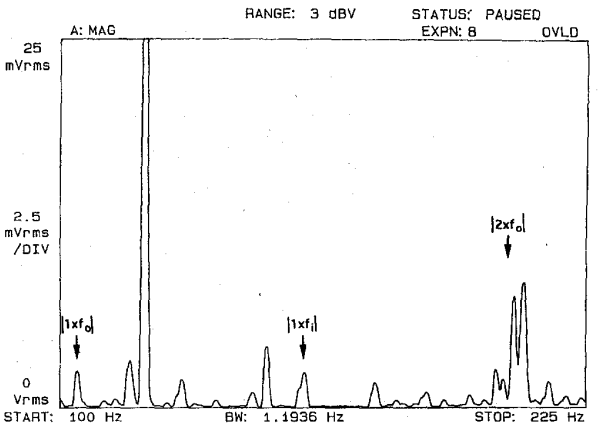


Fig. 9. Vibration spectrum (acceleration) of loaded 4-pole induction machine with brinelling of both bearings (100–225 Hz).

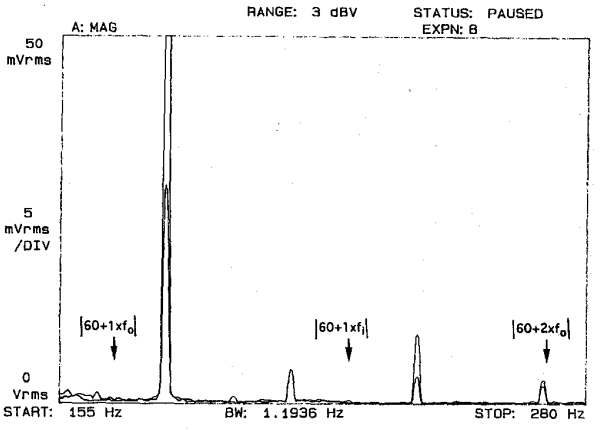


Fig. 8. Stator current spectrum of unloaded 4-pole induction machine with brinelling of both bearings (155–280 Hz).

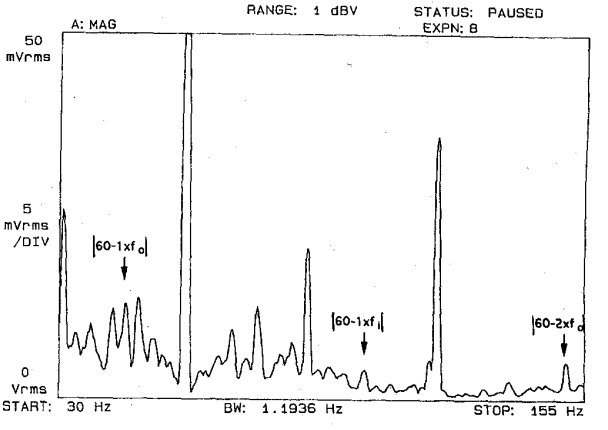


Fig. 10. Stator current spectrum of loaded 4-pole induction machine with brinelling of both bearings (30–155 Hz).

the inner and outer races have the same thickness gives a pitch diameter equal to 60 mm ($PD = 60$ mm). The bearing has nine balls ($n = 9$) with an approximated diameter of 12 mm ($BD = 12$ mm). Assuming a contact angle, $\beta$, of zero degrees and motor operation at the rated shaft speed of 1735 rpm ($f_{rm} = 28.9$ Hz), the characteristic race frequencies of the shaft-end bearing are calculated from (4) and (5) to be $f_o = 104$ Hz and $f_i = 156$ Hz. While these frequencies are based upon the assumptions described above, they provide an indication of the actual characteristic frequencies of the bearing. The same frequencies are predicted when (6) are used.

Because the air gap displacement caused by the damaged bearing is in the radial direction, the radial vibration was measured at the bearing housing using a piezoelectric accelerometer. A linear plot of the vibration spectrum is shown in Fig. 3. It is possible to see the bearing frequency components at one times ($1 \times f_o$) and two times ($2 \times f_o$) the outer race frequency. Because the manufactured bearing damage is limited to the outer race, there is no vibrational component at one times the inner race frequency ($1 \times f_i$). The large spectral component at 120 Hz is produced by the magnetic field of the machine.

Linear plots of the current spectrum are shown in Figs. 4 and 5. Equation (2) predicts the frequencies of interest in the current spectrum to be $|f_e \pm 1 \times f_o|$ and $|f_e \pm 2 \times f_o|$. These current components are indicated on the spectral plots where $f_e = 60$ Hz. The lack of damage on the inner race is indicated by the absence of the predicted inner race frequency components at $|f_e \pm 1 \times f_i|$. It is important to note that the frequency components produced by the bearing defect are relatively small when compared to the rest of the current spectrum. The largest components present in the current spectrum occur at multiples of the supply frequency and are caused by saturation, winding distribution, and the supply voltage. This large difference in magnitude can make detection of the current spectrum bearing harmonics a significant problem.

Brinelling was induced in both bearings as a second type of bearing failure. This bearing failure mode was produced by mounting a denergized induction motor with good bearings on a vibration table. The force of the vibrations caused indentations to be produced in both the inner and outer races of the bearings. These indentations then excited the race frequencies in both the shaft-end bearing (NSK 6208) and the fan-end bearing (NSK 6206). The characteristic race

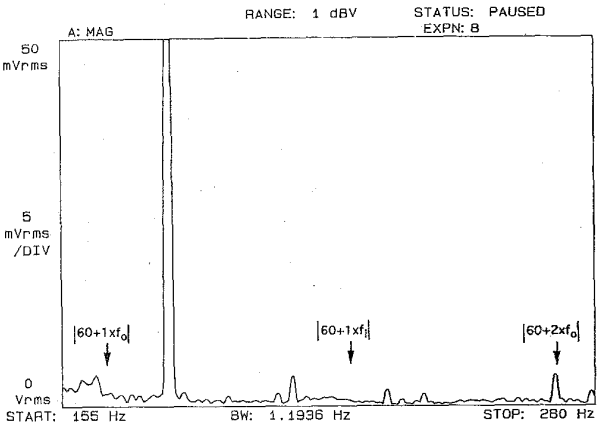


Fig. 11. Stator current spectrum of loaded 4-pole induction machine with brinelling of both bearings (155–280 Hz).

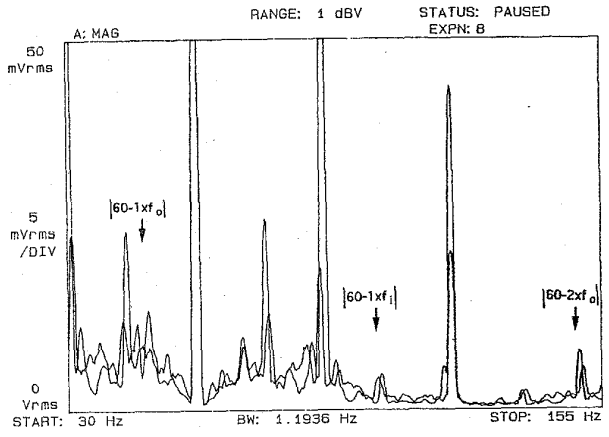


Fig. 12. Stator current spectrums of unloaded and loaded 4-pole induction machine with brinelling of both bearings (30–155 Hz).

frequencies for the shaft-end bearing have previously been calculated to be $f_o = 104$ Hz and $f_i = 156$ Hz. For the fan-end bearing, the bearing data sheet lists the outside diameter of the NSK 6206 at 62 mm and the inside diameter at 30 mm. Averaging gives an assumed pitch diameter of 46 mm ($PD = 46$ mm). The bearing has nine balls ($n = 9$) with an approximated diameter of 10 mm ($BD = 10$ mm). With an assumed contact angle, $\beta$, of zero degrees and motor operation at the rated shaft speed of 1735 rpm ($f_{rm} = 28.9$ Hz), the characteristic frequencies of the fan-end bearing are calculated from (4) and (5) to be $f_o = 102$ Hz and $f_i = 158$ Hz.

Vibration and current measurements were taken on the unloaded, energized motor before and after one month of vibration. These readings were used to evaluate the bearing deterioration over this period of time. The unloaded condition causes the relative speed to be $f_{rm} \approx 30$ Hz which shifts the outer and inner bearing frequencies to $f_o \approx 106$, 108 Hz, and $f_i \approx 162$, 164 Hz for the NSK 6208 and 6206 bearings, respectively. The effect on the mechanical vibration spectrum can be seen in Fig. 6. The vibration levels (measured in terms of acceleration) for the outer race frequencies, $1 \times f_o$ and $2 \times f_o$, and the inner race frequency, $1 \times f_i$, have been increased by the induced bearing damage. This effect is most evident at

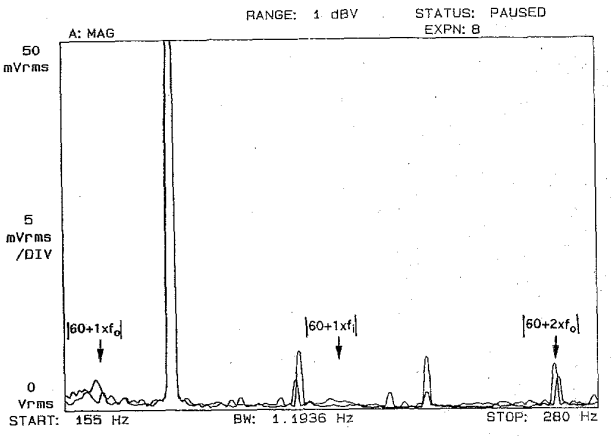


Fig. 13. Stator current spectrums of unloaded and loaded 4-pole induction machine with brinelling of both bearings (155–280 Hz).

$2 \times f_o$ where the outer race frequencies of both bearings form separable peaks.

The same changes are indicated in Figs. 7 and 8 at the predicted current harmonics of $|f_e \pm 1 \times f_o|$, $|f_e \pm 2 \times f_o|$, and $|f_e \pm 1 \times f_i|$. It should be noted that the vibration effect on the stator current is due to the displacement of the rotor with respect to the stator. Therefore, the large differences at high frequencies in the mechanical acceleration levels seen in Fig. 6 are not as significant in the current spectrum. This is clearly illustrated by the relatively large current change at $|f_e - 1 \times f_o|$ and the much smaller changes at $|f_e \pm 2 \times f_o|$ even though the mechanical vibration spectrum (acceleration) of the test machine suggests the opposite effect.

The current and vibration measurements for the damaged bearings were repeated under full load operation of the induction machine. The effect of the loading can be seen in the vibration spectrum of Fig. 9. The amplitudes of the bearing vibrations have decreased because of the damping produced by the mechanical load. The current harmonics predicted for rated speed operation can still be found in the current spectrums of Figs. 10 and 11. This indicates that, regardless of the load level of the machine, the bearing components are still detectable in the current spectrum.

The predicted current components are emphasized by plotting the unloaded and loaded phase current spectrums on the same graph. The speed difference caused by the two load levels shifts the bearing frequency components. This effect is clearly seen in the stator current spectrum of Figs. 12 and 13. The damping effect of the load is also emphasized in these shifted current components.

## V. Conclusions

This paper has investigated the feasibility of detecting bearing faults using a spectrum of a single phase of the stator current of an induction machine. Air gap eccentricities cause variations in the air gap flux density that produce visible changes in the stator current spectrum at predictable frequencies. Since rolling-element bearings support the rotor, a bearing defect also produces variations is the air gap length of the machine. These variations generate noticeable changes

in the stator current spectrum. The predictability of air gap eccentricities has been extended to include faults in rolling-element bearings that excite mechanical vibrations at fractional values of the rotational speed. Measured current and vibration spectrums were presented to verify this relationship. While these changes are relatively small when compared to the rest of the current spectrum, they fall at locations that are different from the supply and slot harmonics of the machine. With sufficient spectral resolution, this discrimination makes the bearing harmonics sufficiently distinct for use as effective indicators of rolling-element bearing damage.

## ACKNOWLEDGMENT

The authors would like to acknowledge the support provided by S. Farag of Siemens. His assistance was greatly appreciated.

## REFERENCES

[1] P. F. Albrecht, J. C. Appiarius, R. M. McCoy, E. L. Owen, and D. K. Sharma, "Assessment of the reliability of motors in utility applications—Updated," *IEEE Trans. Energy Conversion,* vol. EC-1, no. 1, pp. 39–46, Mar. 1986.

[2] IAS Motor Reliability Working Group, "Report of large motor reliability survey of industrial and commercial installations:, Part I," *IEEE Trans. Ind. Applicat.,* vol. IA-21, no. 4, pp. 853–864, July 1985.

[3] M. E. Steele, R. A. Ashen, and L. G. Knight, "An electrical method for condition monitoring of motors," in *Int. Conf. Elec. Mach.—Design and Applicat.,*July 1982, no. 213, pp. 231-235.

[4] G. B. Kliman and J. Stein, "Induction motor fault detection via passive current monitoring," in *Proc. Int. Conf. Elec. Mach.,* Aug. 1990, pp. 13–17.

[5] ——, "Methods of motor current signature analysis," *Elec. Mach. Power Syst.,* vol. 20, no. 5, pp. 463–474, Sept. 1992.

[6] P. Eschmann, L. Hasbargen, and K. Weigand, *Ball and Roller Bearings: Their Theory, Design, and Application.* London: K. G. Heyden, 1958.

[7] J. Riddle, *Ball Bearing Maintenance.* Norman, OK: Univ. of Oklahoma Press, 1955.

[8] R. R. Schoen and T. G. Habetler, "Effects of time-varying loads on rotor fault detection in induction machines," in *Conf. Rec. 28th Annu. IAS Meeting,* Oct. 1993, pp. 324–330.

[9] R. K. Mobley, *An Introduction to Predictive Maintenance.* New York: Van Nostrand Reinhold, 1990.

[10] R. L. Schiltz, "Forcing frequency identification of rolling element bearings," *Sound and Vibration,* pp. 16–19, May 1990.

**Randy R. Schoen** (S'88–M'94) received the B.E.E., M.S., and Ph.D. degrees in electrical engineering from the Georgia Institute of Technology, Atlanta, GA in 1989, 1990, and 1994, respectively. His research while at Georgia Tech addressed the problem of failure prediction in line-operated three-phase induction machines using current-based spectral analysis.

Since 1994, he has been employed by the Louis Allis Company, Milwaukee, where he is involved in electric machine design and research. He has published several papers.

Dr. Schoen is a member of the IEEE Industry Applications, Power Engineering, and Power Electronics Societies, and serves on the IAS Electric Machines Committee. He received a prize paper award in 1994 from the IEEE Industry Applications Society.

**Thomas G. Habetler** (S'82–M'83–S'85–M'89–SM'92) received the B.S.E.E. degree in 1981 and the M.S. degree in 1984, both in electrical engineering, from Marquette University, Milwaukee, WI, and the Ph.D. degree from the University of Wisconsin-Madison, in 1989.

From 1983–1985, he was employed by the Electro-Motive Division of General Motors as a Project Engineer. While there, he was involved in the design of switching power supplies and voltage regulators for locomotive applications. He is currently an Assistant Professor of Electrical Engineering at the Georgia Institute of Technology. His research interests are in switching converter technology and electric machine protection and drives.

Dr. Habetler was co-recipient of the 1989 first-prize paper award and the 1991 second-prize paper award of the Industrial Drives Committee, and the 1994 second-prize paper award of the Electric Machines Committee of the IEEE Industry Applications Society. He serves as Associate Editor of the IEEE TRANSACTIONS ON POWER ELECTRONICS. He also serves as Secretary of the IEEE Power Electronics Society.

**Farrukh Kamran** (S'94) received the B.Sc. degree in electrical engineering from the University of Engineering and Technology, Lahore, Pakistan, in January 1988. He earned the M.S.E.E. degree from the Georgia Institute of Technology, Atlanta, in December 1992. He is currently pursuing the Ph.D. degree in electrical engineering at Georgia Tech. He is engaged in rsearch on controlled rectifiers, active power filters, line conditioners, and UPS's.

After graduating with the B.Sc. degree, he served as design engineer with EGS (pvt) Ltd., Pakistan, from 1988 to 1989. He joined HiPo Electronics (pvt.) Ltd., Pakistan, in 1989 as a senior design engineer in power electronics, where he served until 1991.

Mr. Kamran was awarded a scholarship for graduate studies by the Government of Pakistan. He is a member of the Pakistan Engineering Council.

**Robert G. Bartheld** (SM'70) is a native of La Crosse, WI. He received the B.S.M.E. from Iowa State University in 1951 and took postgraduate courses at the University of Cincinnati.

Now retired after 41 years with Siemens Energy & Automation, he is doing some consulting work in the electric motor field. While with SE&A he held positions of Engineering Manager of the Motor Division and Corporate Manager of Technology Transfer. He holds 7 patents and has authored numerous technical articles. He has been engaged in motor standards activities for over 30 years.

Mr. Bartheld is a past Chairman of NEMA Motor & Generator Section. In 1990, he received the NEMA Kite and Key Award for his contributions to NEMA and the electroindustry. He is a past chairman of ISO/TC108, Mechanical Shock, and Vibration. He is currently the Technical Adviser to the U.S. National Committee to IEC for Rotating Electrical Machines and is Secretary to IEC/TC98 Electrical Insulation Systems.